Annals of R.S.C.B., ISSN:1583-6258, Vol. 25, Issue 3, 2021, Pages. 8420 - 8434
Received 16 February 2021; Accepted 08 March 2021.

Synthesis of Magnetic Poly (Thiourea-Amide) Chelating Resin and its Absorption Behavior Towards Pb(II) and Cd(II)ions

Iman Saad Ali[1*], T.E. Jassim[2], M.S.H. Hussain[3]

[1*]College of Education for Pure Science, University of Basrah, Iraq. E-mail: imansaad086@gmail.com
[2]College of Education for Pure Science, University of Basrah, Iraq.
[3]College of Education for Pure Science, University of Basrah, Iraq.

ABSTRACT

In this work, a novel magnetic nanocomposite based on aromatic benzoylthiourea as a nanocomposite polymer was synthesized via reaction of substituted amine and terephthalodiisothiocyanate which is obtained by the reaction of terephthaloyl dichloride and potassium thiocyanate. As the phase transfer catalyst, poly(ethyleneglycol400) was tested. Substances 1HNMR, 13CNMR, Elemental analysis were characterized. Thermal properties of obtained polymer (PO) were examined by using TGA-DTG, The polymerization reaction was carried out via surface modification of magnetic nanoparticles (Fe3O4 MNPs) using polymerization process. Various analytical techniques such as field-emission scanning electron microscopy (FE-SEM), transmission electron microscopy, X-ray, and vibrating sample magnetometer (VSM) analyses were used to confirm the structure of the prepared nanocomposite. A sphere morphologies were observed by FE SEM images by the result of polymerization process and fabrication of the synthetic polymeric strands on the surface of the modified Fe3O4 magnetic cores. Surface area of magnetic benzoylthiourea polymers was measured by using the BET. The application of this novel magnetic nanocomposite was applied comparatively The elimination of Ni (II) and Cd(II)ion from aqueous solutions of experimental conditions and parameters including pH, adsorbent dosage, contact time for the removal of heavy metals has also been investigated and antioxidant activities, including the operation of DPPH radical scavenging, were evaluated in vitro, indicating that the poly amid displayed important antioxidant activities.

KEYWORDS

Poly, Thiourea-Amid, Magnetic, Nanoparticles, Adsorbent, Antioxidant.

Introduction

Pollution has allowed various contaminants to enter the ecosystem, which has accelerated the transport of contaminants in the food chain and increased the risk to living organisms. Currently > 22 per cent of diseases and 23 per cent of deaths are due to environmental contamination (Wen,2019) Industries are key players in the national economies of many developing countries, but unfortunately they are also the major polluters of the environment. Industrial wastewater discharged from different industries is considered a major source of environmental pollution (soil and water) among the various sources of environmental pollution (Goutam SP, Saxena,2018, Saxena2017) Industrial wastewater contains a variety of organic and inorganic pollutants that can cause serious environmental pollution and health hazards (Bharagava,2017). Metal ions in waste disposal from various sources have become an ecotoxicological hazard. The pollution of heavy metals pollutes underground water, which affects human plants and animals. Some heavy metals are necessary for the growth of plants and microorganisms, but they become poisonous beyond certain concentrations. The removal of lead(II) and cadmium ions from the effluent is therefore significant in order to protect the environment and living being (Murugesan,2014). A lot of work has therefore been done to solve the problem of heavy metal pollution in wastewater. Conventional treatment technologies are the chemical precipitation method, the electrolytic process, the ion exchange method and the adsorption method; among these methods, adsorption is generally preferred for the removal of heavy chelating resins as an adsorbent material that has the advantage of high adsorption capacities, easy to be separated and reusable (Huang,2017). Thiourea and its derivatives have found many applications in analytical chemistry, heterocyclic metal flotation, leaching and extraction, rubber processing and many others. Particularly interesting group of thiourea derivatives are acylthioureas due to simple synthesis, stability and biological activity. The heavy metal ions are soft Lewis acids and the thiourea derivatives are soft Lewis bases, according to Pearson's HSAB theory, so they are likely to form tight coordination bonds. Extensive experiments are also being carried out to investigate the chemistry of these organisms. It is very important because heavy metal compounds are highly toxic to living organisms and can assist in human detoxification through chelating (Okuniewski, 2015). As strong support materials, magnetic nanoparticles (MNPs) with high surface areas such as nanoscale magnetite (Fe3O4) have been considered. Due to their high adsorption power, short adsorption time and the simple separation of metal-loaded MNPs by applying an external magnet, surface modified MNPs with unique functional groups such as diamines have been tested for removal of heavy

Annals of R.S.C.B., ISSN:1583-6258, Vol. 25, Issue 3, 2021, Pages. 8420 - 8434
Received 16 February 2021; Accepted 08 March 2021.

metals. On the other hand, functional groups containing donor atoms of sulfur and nitrogen are highly selective against precious metals, based on Pearson's theory of hard and soft acids and bases (HSAB theory) (Lin,2013, Pearson,1968) The chelating resin is a good candidate for use as support for the metal oxide nanoparticles MONPs since chelating resins have been reported to exceed both cation and anion exchange resins in the removal of metal from solutions. Not only can chelating resins bind metal ions through their sites of ion exchange, but they can also bind them through coordination with their ligand atoms, A feature that is absent from both cation and anion exchangers. It was therefore anticipated that supporting MONPs on chelating resins could generate composite adsorbents from wastewater with excellent metal removal efficiency (Dlamini, 2020).

In this work, we have intended to synthesize polymers in the backbone of its structure carrying multifunctional groups. By the reaction of terephthaloyl chloride with 4.4'-diaminodiphenyl ether compound with two active functional groups, this design could be carried out with the use of catalyst and the achievement of the polymerization reaction on the surface of functionalized Fe3O4 MNPs is propounded Scheme 1), as well as the characterization of the proposed magnetic nanocomposite based on p diaminodiphenyl ether and its antioxidant activities and targeted to examine the ability of the resulted polymers to function as efficient adsorbents in removing some heavy metal ions from aqueous solutions under various conditions.

Experimental Work

Instrumentation

FT-IR measurements were recorded on Shimadzu model FTIR-8400S. 1H NMR and 13C NMR spectra were obtained with Bruker spectrometer model ultra-shield at 400 MHz. The results were recorded using tetramethylsilane (TMS) as internal standard and DMSO-d6 as solvent. Chemical shifts are given in δ scale (ppm). Atomic absorption data were obtained with the aid of a Phoenix-986 AA spectrophotometer. Note: in some 1H NMR spectra, the peaks at chemical shifts 2.5 and 3.35 are for the solvent (DMSO-d6) and dissolved water in (DMSO-d6), respectively.

All the chemicals used in this work were purchased from sigma- Aldrich and used it is without further purification.

Synthesis of Terephthaloyl Chloride T- Cl

At ambient temperature, a mixture of terephthalic acid (1.66 g, 10 mmol), 4 mL of SOCl2, and a few drops of DMF were mixed for 4 h. The resulting solution was filtered and vacuum-concentrated. The crude product was dissolved in CH2Cl2 and concentrated to extract unreacted SOCl2 again under vacuum. Finally, after recrystallization of dichloromethane/ petroleum, a white solid was obtained, after it was recrystallized from dichloromethane/ petroleum ether (1/3, v/v). Yield: 85%. The synthesis of T-Cl is described in Supplementary Content, with a yield of 85%. (Zhou, 2017).

Synthesis of Terephthaloyldiisothiocyanate

Terephthaloyldiisothiocyanate was synthesized according to the literature report (Zhou,2017) (0.02 mol,2.0g) potassium thiocyanate and (0.01mole 2g) terephthaloyldichloride was dissolved in dichloromethan1 mL Poly(ethyleneglycol400) was added. After 2 h stirring at room temperature, the mixture was filtered and precipitate (potassium chloride) was removed. 30 mL terephthaloyldiisothiocyanate solution was obtained.

Synthesis of Poly N1-ethanethioyl-N4-((4-(4 (Methylamino) Phenoxy) Phenyl) Carbamothioyl) Terephthalamide (PO)

diisothiocyanate filtrates was added by dropwise method into solutions which contain 4.4′-diaminodiphenyl ether of appropriate concentrations in30 ml methylenechloride. Poly(ethyleneglycol400) was added to each reaction solutions as a phase transfer catalyst. The reaction solutions were stirred under reflux 6h. The yellow precipitated polymer was filtered, washed several times with methylenechloride, water and diethylether and dried at $^{\circ}$C 100 (Huang, 2017). Elemental analysis calculated for (C24H22N4O3S2): C, 60.2, %; H, 4.01%; N, 11.71,S,13.40%. Found: C60. 3%; H, 3.96%; N, 10.95%,S,11.2.

The synthetic route of PO was represented as Scheme 1.

Annals of R.S.C.B., ISSN:1583-6258, Vol. 25, Issue 3, 2021, Pages. 8420 - 8434
Received 16 February 2021; Accepted 08 March 2021.

Fig. 1. The synthetic route of PO

Preparation of Fe3O4 NPs

Fe3O4 NPs was prepared by the improved co-precipitation method according to the previously reported.29,30 Typically FeCl3•6H2O (5.41 g, 20 mmol) and FeSO4•7H2O (2.78 g, 10 mmol) were dispersed and dissolved in 80 ml DI water, then the pH was adjusted to 10.5 by ammonia solution. After that the solution was heated to 68 °C and maintained for 12 h in water bath with constantly stirring. Finally, the resulting brown-black product was purified by filtration, washed by DI water (Bandar, 2020).

Preparation of Aromatic Thiourea - Amid/Magnetic Fe3O4 Nanoparticles

In a 250 ml flask aromatic poly thiourea-amide (0.5 g, see Sketch 1) was dissolved in N, N´-di-methyl formamide (DMF) (100 ml) under an N2 atmosphere. The Fe3O4 nanoparticle/DMF suspension (100 ml) as prepared above was added drop-wise to the polymer solution over a period of 60 min, whilst the polymer solution over a period of 60 min, whilst stirring vigorously and ultrasonic ting under argon atmosphere. The suspension was stirred for a the 24 h at room temperature, then placed on a neodymium magnet to precipitate the magnetic particles. (Wei, 2006). The particles were washed further with methanol and dried at room temperature in vacuum oven.

Annals of R.S.C.B., ISSN:1583-6258, Vol. 25, Issue 3, 2021, Pages. 8420 - 8434
Received 16 February 2021; Accepted 08 March 2021.

Results and Discussion

Synthesis

The new polymer in this study were synthesized by reaction of terephthaloyl dichloride with potassium thiocyanate in CH2Cl2 in a 1:2 mole ratio at a good yield (90 percent). The precipitated salt (KCl) was isolated by filtration and the filtrate (terephthaloyl isothiocyanate solution in dichloromethane) was treated at room temperature with 4.4'-diaminodiphenyl ether in a 1:1 mole ratio continuously stirring for 6 hrs.. Scheme (1). By elemental analysis, C, N and S percentages were obtained, and the results are summarized in Table 1. The percentages of sulfur in the thiourea compound elemental analysis data are typically lower than their theoretical value. This is the cause of thiol tautomerism formation and hydrogen sulphide (H2S) degradation (Androvič, 2016). The Organosolubility of PO, Poly(thiourea-amide) was found to be highly soluble at room temperature in typical organic polar solvents such as DMAc, DMSO, NMP, DMF and THF (Table 1). Polymer solubility (10 mg) was tested at room temperature in various solvents (1mL). High solubility is generally a prerequisite for polymer processing. The existence of flexible groups of thiourea in polymer backbone can be attributed to the good Organosolubility of poly thiourea-amides. The presence of a flexible ether group in the spine had a beneficial effect on the solubility of poly (thiourea-amide).

It was found that (1.02 dL/g) thiourea was the inherent viscosity of the poly(thiourea-amide) measured in DMF.

The poly(thiourea-amide) with p-linkages (PO) included the maximum ηinh of 1.02 dL/g. The poly(thiourea-amide) with p-linkages (PO) had higher suggesting polymer chain rigidity. Higher rigidity can be related to the highest ηinh of PO; a high degree of inter-chain hydrogen bonding associated with greater chain symmetry and efficiency of packing. To evaluate the molecular weight of PO, the above claim was confirmed by the GPC calculation. Table 1 synthesized polymer displays the GPC-determined weight-average molecular weight (Mw) and polydispersity index (PDI=Mw/Mn) The Mw and PDI suggested a relatively high molecular weight of the PO bearing C=S.

Table 1. Average molecular weight (Mn), average molecular weight (Mw), polydispersity index (PDI), ηinh of the and elemental analysis results S Calc/Found

Compounds	Mw	Mn	PDI	ηinh	%C	%H	%N	%
PO	64400	378820	1.7	1.02	60.23 (60.45)	4.61 (4.57)	11.7 (11.34)	13.4 (11.3)

Table 2. Solubility of poly(thiourea-amid)

Solvent	**Solubility**	**Solvent**	**Solubility**
N, N-dimethylacetamide DMAc	++	Tetrahydrofuran	+
Dimethyl sulfoxide DSMO	++	Acetone	-
N-methyl-2-pyrrolidoneNMP	++	methanol	-
N,N´-di-methyl formamide DMF	++	m-Cresol-	-
Chloroform	+	Pyridine	+

Solubility: (+ +) soluble at room temperature, partially soluble (+), and (-) insoluble

IR and NMR Spectra

The FT – IR spectrum of both monomer(T-Cl) and polymer (PO), The spectrum of monomer showed the of stretching vibration of terephthalic carbonyl (C=O) which usually appeared at high frequency 1768 $cm^{-1}$and (C-H) for aromatic ring at 3039cm-[1.]

The spectrum of polymer PO also showed characteristic bands at 3099 cm^{-1}, 1674 cm^{-1}, 1602 cm and 1143 cm^{-1} could be assigned for stretching vibration of N–H, C = O (amide), C=N, and C=S groups respectively. (Huang, 2017)

Annals of R.S.C.B., ISSN:1583-6258, Vol. 25, Issue 3, 2021, Pages. 8420 - 8434
Received 16 February 2021; Accepted 08 March 2021.

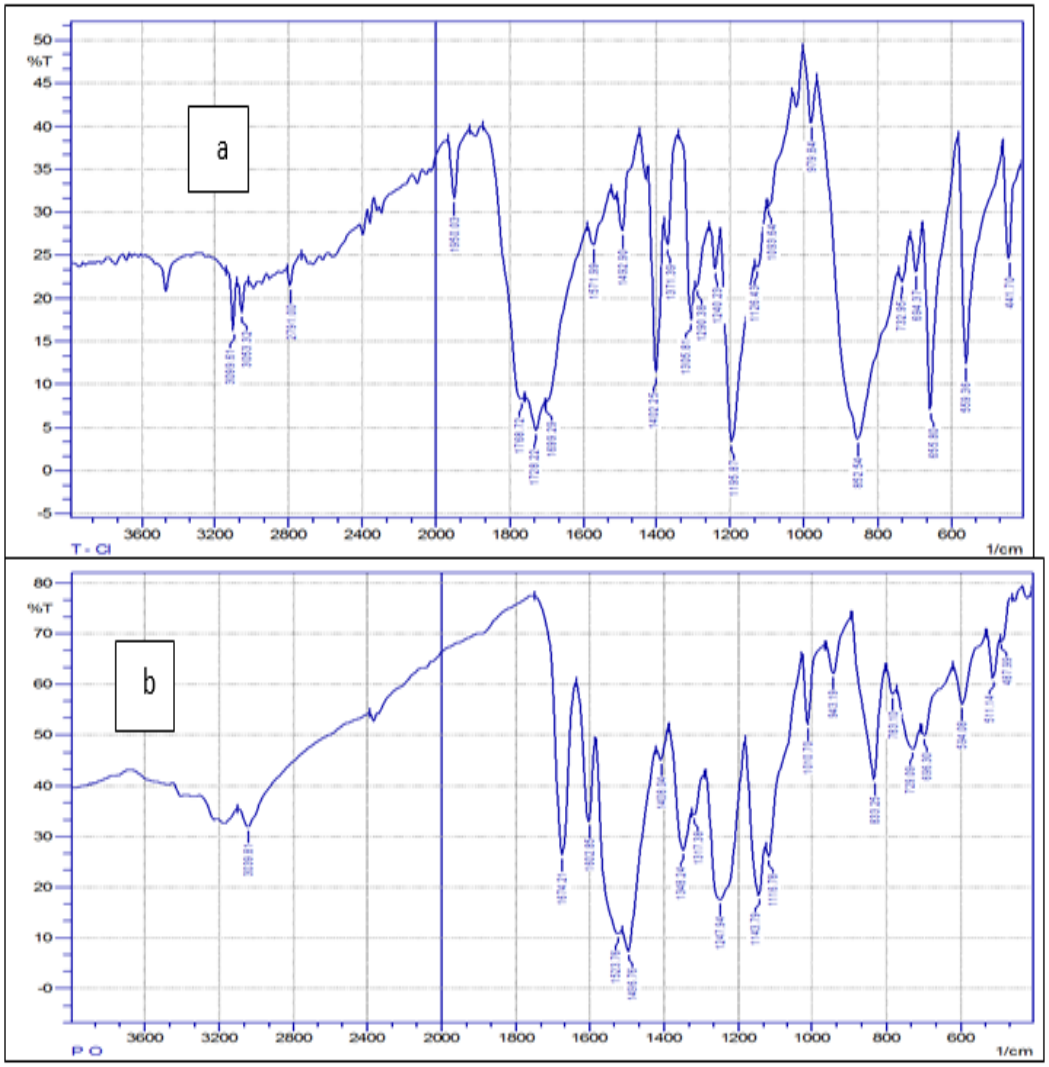

Fig. 2. FTIR spectra of (a)T-Cl, (b) PO

The H-NMR spectrum of monomer T-Cl, Fig.(2a) showed a multiple signal between (δ= 8.12ppm), assigned to protons of the aromatic ring.

13C NMR spectra of the of monomer T-Cl shown in. Fig.(2b) The structures are confirmed by the presence of phenyl carbons (3,4.1,6) at 129–133 ppm and at 135 ppm for 3,5, carbonyl C=O 166 ppm (Zhou, 2017).

The H- NMR of polymer PO (Fig. 3, a) showed characteristic H NMR were recorded using DMSO-d6 solvent. 1H NHA signals at 12.42 and NHB signals at11.66 ppm respectively. In the other hand a multiple signal between (δ= 6.70–8.09 ppm), assigned to protons of the aromatic ring.

Fig.3b, C13-NMR spectra of PO shown in were recorded at solid phase. The structures are confirmed by the presence of phenyl carbons (-C=C-) at121–142 ppm and thiocarbonyl group C=S signal at190. 74 ppm, carbonyl C=O 169.97 ppm and signal at 152.12ppm C-O. (Abd Halim, et al. 2016).

Annals of R.S.C.B., ISSN:1583-6258, Vol. 25, Issue 3, 2021, Pages. 8420 - 8434
Received 16 February 2021; Accepted 08 March 2021.

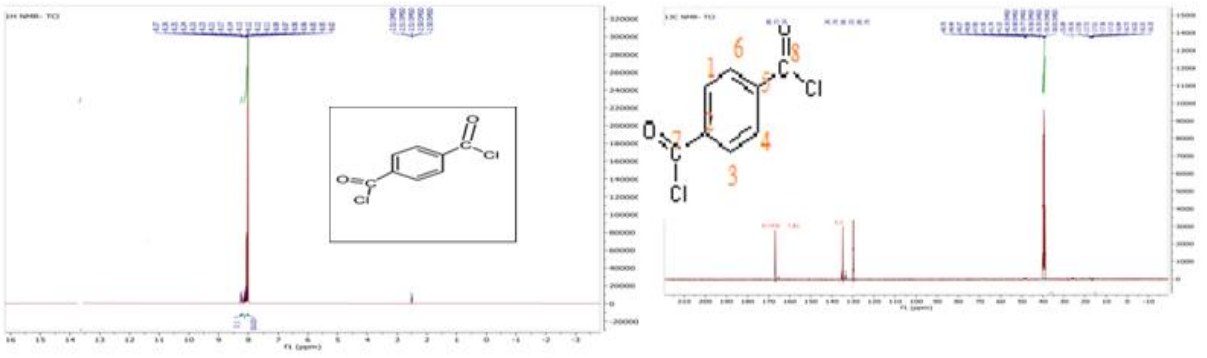

Fig. 3. a. H- NMR. **b.** C13 NMR for T-Cl

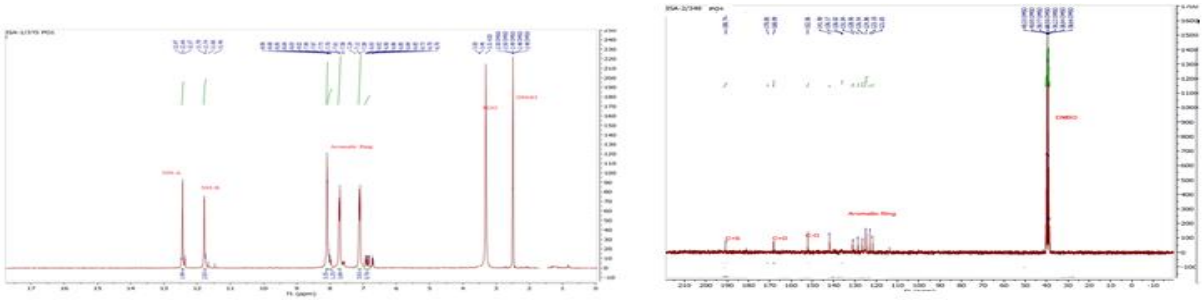

Fig.4. a. H-M=NMR. **b.** C13 NMR for PO

Thermal Properties

The thermal properties of the polymer (PO) was investigated by TGA/DTG and the weight loss curve is presented in Fig The initial decomposition temperature (T0) was about 336^{o}C, (T50) was about 570^{o}C and the maximum decomposition temperature (T max) was found in 586^{o}C along with char yield of PO around 25.54 %. Moreover, PO illustrated three decomposition steps from 300–600^{o}C indicating a complex degradation mechanism. In 4.4'-diaminodiphenyl ether ODA, the flexible thiourea group and electrophilic oxygen atom allowed looser molecular packaging and resulted in enhanced solubility in organic solvents without degrading PO thermal properties (Şenol, 2019). (The thermal properties of the polymer (PO.) FIG.5.

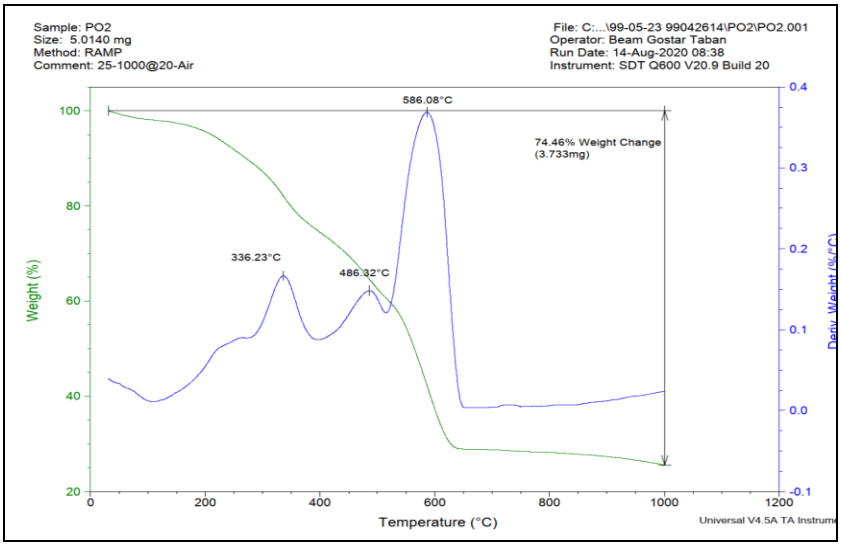

Fig. 5. The thermal properties of the polymer (PO)

Annals of R.S.C.B., ISSN:1583-6258, Vol. 25, Issue 3, 2021, Pages. 8420 - 8434
Received 16 February 2021; Accepted 08 March 2021.

- **XRD**

The XRD results of pure Fe3O4, polymer and PO/Fe3O4 are shown in Fig. 6 which confirmed the components of the iron oxide particles. Six characteristic peaks for Fe3O4 (2Θ = 30.44◦, 35.77˚, 43.44 ◦, 53.84◦, 57.400◦, and 62.9◦), marked by their indices ((2 2 0), (3 1 1), (4 0 0), (4 2 2), (5 1 1), and (4 4 0)), were observed in both samples. These results indicated that the magnetic substance of PO was validated as Fe3O4 (Li, X el at, 2012).

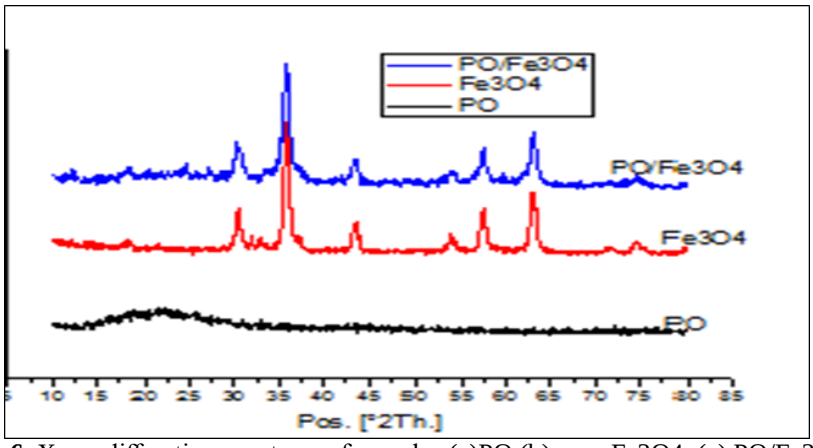

Fig.6. X-ray diffraction spectrum of samples (a)PO (b) pure Fe3O4, (c) PO/Fe3O4

Magnetic Properties of Magnetite NPs and Polymer

The magnetization curves measured at room temperature for pour Fe3O4 MNPs and Fe3O4 MNPs coated with PO are compared in Figure 7. For both samples, there was no hysteresis in the magnetization, indicating that the magnetic particles formed are superparamagentic. This can be due to the small size of NPs greater than the super critical paramagnetic size (25 nm). On the other hand, when the particles' magnetic component size is smaller than the critical size, the particles would be superparamagnetic. The magnetization value of saturation was estimated at 74.40 emu g^{-1} for Fe3O4 and 50.60 emu g^{-1} for Fe3O4 coated with PO. The excellent crystal structure was demonstrated by the high saturation magnetization of pure Fe3O4. The PO coated Fe3O4 saturation magnetization values were lower than the value for pure magnetite nanoparticles, Therefore, after coating polythiourea-amid the surface of Fe3O4 MNPs, the saturation magnetization was decreased. This was due to the presence of the magnetite nanoparticles covering the diamagnetic shell that quenched the magnetic moment (Kirupha,2012). Nevertheless, both showed super paramagnetic behaviors.

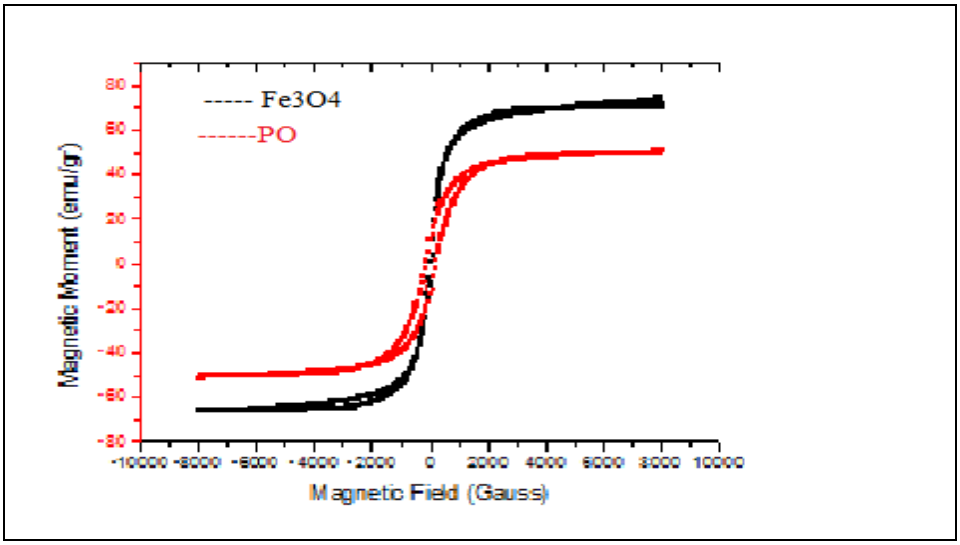

Fig. 7. Field dependence of magnetization for the Fe3O4 (a) and PO/Fe3O4 (nanocomposite (b)).

Annals of R.S.C.B., ISSN:1583-6258, Vol. 25, Issue 3, 2021, Pages. 8420 - 8434
Received 16 February 2021; Accepted 08 March 2021.

FT-SEM

FT-SEM is a useful method to research the basic surface morphology of materials such as porosity, particle shape, and the distribution of nanoparticles in the matrix to the required size. The SEM images of the Fe3O4 nanoparticles synthesized are shown Figure (8a) displays spheres with a mean diameter of 23 nm in the FT-SEM picture of the iron oxide nanoparticles obtained by the co-precipitation process. Nanoparticles that have been synthesized and agglomerated into comparatively larger spheres with a mean diameter of around 24 nm. in the figure (8a) the FT-SEM image of iron oxide nanoparticles obtained by the co-precipitation method shows spheres with a mean diameter of 23 nm. Synthesized nanoparticles that have agglomerated into relatively larger spheres with a mean diameter of around 24 nm. Surface morphology of raw polymers is shown in (Fig. 8b) The resin morphology provides details on the topology of the surface and the defect of the structure. It was, clearly, seen in Fig. 8.b) SEM photos that are amorphous and have a significant number of platelet-like units of the raw polymer resin. Typically, polymers with an aromatic substituent pendant lead to the formation of an amorphous. In Figure (8c,d). PO/Fe3Obefor and after adsorption this observation indicates that it can be inferred that certain amide groups, thiourea and aromatic rings and their interactions, such as heavy hydrogen bonds and van der Waals interactions with Fe3O4 nanoparticles, proximity and adhesion should be observed due to the presence of different functional groups in PO/Fe3O4 (Bandar, 2020).

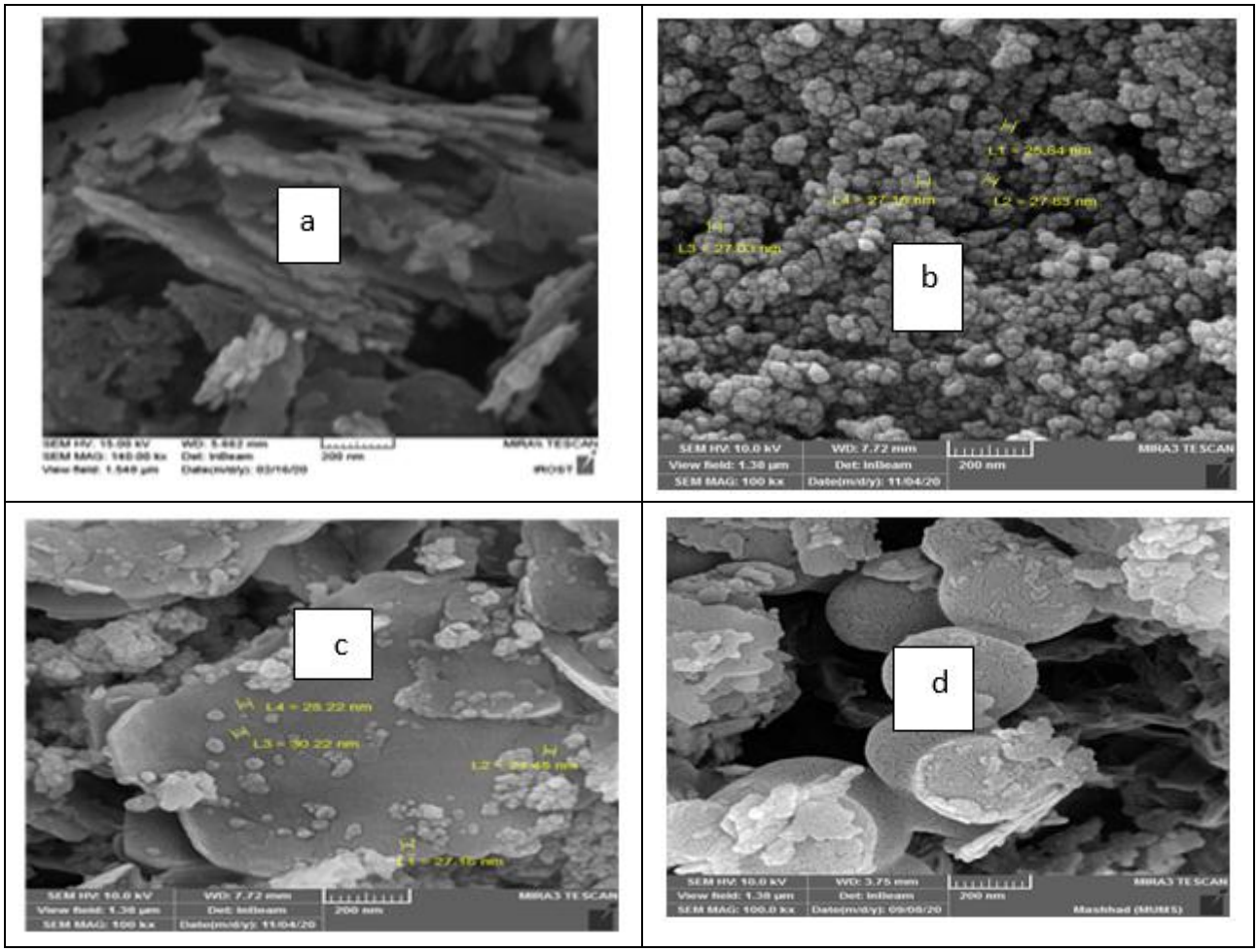

Fig. 8. FT-SEM image of (a) PO, (b) Fe3O4, (c) PO/Fe3O4, (d) PO/Fe3O4 after Adsorption

TEM and Size Distribution

TEM analysis of the NPs showed that both Fe3O4 and Fe3O4 NPs were approximately non spherical in shape. Fig. 9 a displays TEM images of Fe3O4 NPs with sizes from 10 to 14 nm and an average of 12.8 nm in diameter and fig (9b) shows Fe3O4 NPs coated with a thin layer of polymer (PO/Fe3O4 core/shell). Particle sizes are in the range of

Annals of R.S.C.B., ISSN:1583-6258, Vol. 25, Issue 3, 2021, Pages. 8420 - 8434
Received 16 February 2021; Accepted 08 March 2021.

45–65 nm in addition, the images have shown that the polymer coating is almost homogeneous. Fig. 9(a) shows the size distribution of Fe3O4 NPs ethanol dispersion, it has a narrow size distribution in the range of 10 to15 nm with an average size of 12.8 nm. Fig. 9b shows the size distribution of the dispersion of PO4/Fe3O4 NPs, has a large size distribution in the range of 30 to 80 nm. nm most of the particles size was less than 100 nm with average size of 50 nm, which is consistent with the size determined, using TEM (Magdalena,2018).

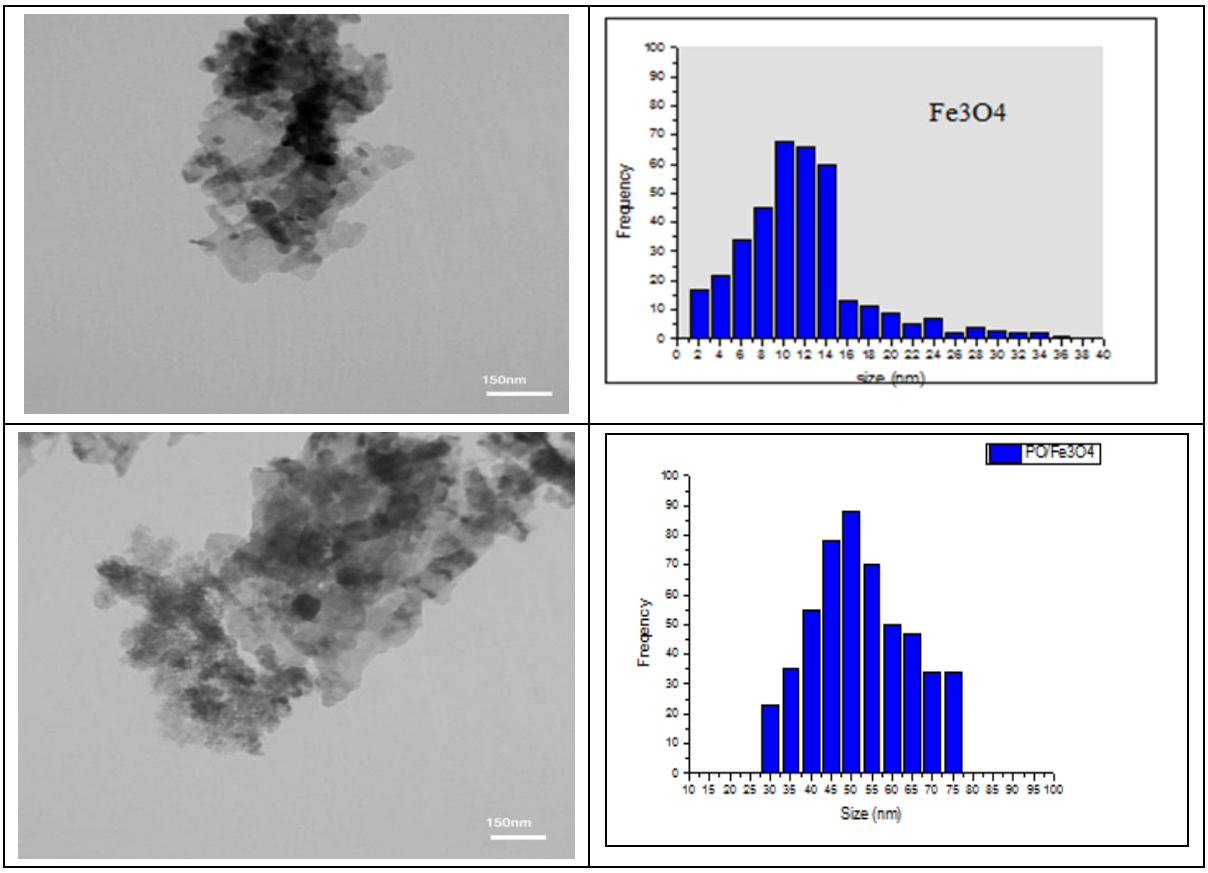

Fig. 9. TEM and size distribution of (a) Fe3O4, (b) PO/Fe3O4

Nitrogen Adsorption-desorption Analysis

According to IUPAC notation, microporous, mesoporous and macroporous materials have pore diameters of 2 nm > D, 2 nm < D < 50 nm and D > 50 nm respectively. The resulting nitrogen adsorption desorption isotherms of poly amid nanocomposite be categorized as type-IV isotherms by IUPAC classification with narrow hysteresis indicating the presence of mesopores). Modification with thiourea derivatives and polymeric materials appears to be reducing the surface area of natural adsorbents and increase their pore size. When pores have small size, specific surface area has increased. Because, specific surface area de pends on the size of the pores. Mesoporosity is affected by chemical and termal processes. One of the most important properties of porous solids is their adsorption capability Here, the effect of modification of thiourea derivatives on polymer surfaces was investigated. The specific surface area of the PO/Fe3O4 nanocomposite has been determined by BET. The BJH pore size distribution plot and the N2 ad sorption-desorption isotherm of the PO/Fe3O4 nanocomposite are shown in Fig. 10. The specific surface area, the total pore volume and the estimated average pore diameter of the nanocomposite were 111.555 $m2g^{-1}$,0.0841 $cm3g^{-1}$ and 29.134 nm, respectively (Cai, 2019, Fu Y, 2018, Chen D, 2019).

Annals of R.S.C.B., ISSN:1583-6258, Vol. 25, Issue 3, 2021, Pages. 8420 - 8434
Received 16 February 2021; Accepted 08 March 2021.

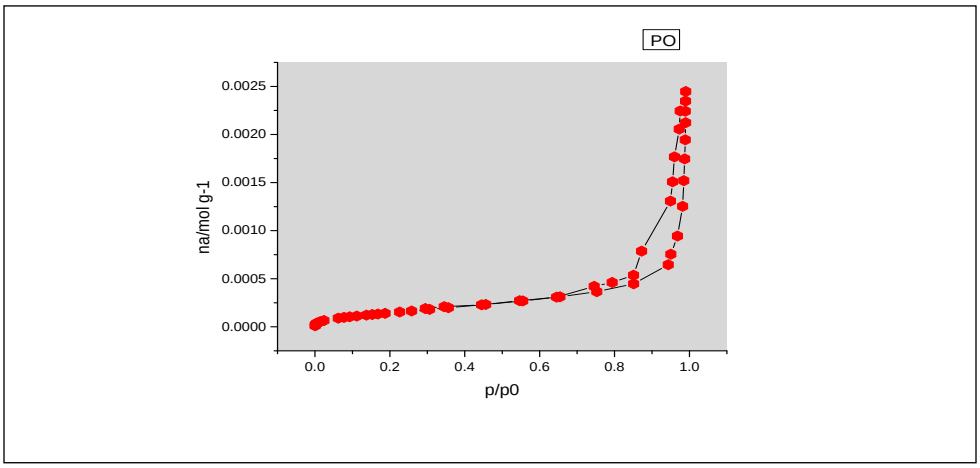

Fig. 10. Nitrogen adsorption-desorption

Metal ions Removal Studies by the Synthesized Polymer (PO)

The removal efficiency by adsorption of the studied heavy metal ions was carried out on the newly synthesized polymer PO/Fe3O4. A detailed analysis of different parameters affecting the adsorption process was carried out, including contact time, solution pH, polymer weight. Batch adsorption experiments were carried out by shaking the flasks at 190 rpm for a constant period of time using a horizontal bench shaker. Following a systematic process the removal of heavy metal ions from aqueous solutions by the use of PO/Fe3O4 in a batch system was studied in the present work. The data obtained in batch studies were used to calculate the percentage removal of heavy metal ions by using the following mass balance relationship:

Adsorption capacity (mg/ g) calculated using the following relationship:

$$qe = (Co – Ce)V/W$$

Where Co and Ce are the initial and final adsorbate concentrations (mg/L) V is the volume of the adsorbate solution (mL) and W is the mass of the adsorbent (mg) the studies were carried out with initial concentration (100 mg/ L) for Cd^{+2} and Cd^{+2} ions, the mass of the adsorbent (10mg)/ 10ml.

Batch Studies

Influence of pH on the Sorption of Pb(II) and Cd(II) The removal of metal ions by adsorption from the aqueous solution is highly dependent on the solution's pH, which influences the adsorbent's surface charge and the degree of ionization. The experimental results for Pb+2 and Cd+2 removal under different initial solution pH values at adsorption equilibriums are shown in Fig 11.

For the adsorbents PO/Fe3O4 the pH values ranged from 2 to 7 It shows that the adsorption capacity increases dramatically with increase of pH and over a pH value of 6, the adsorption capacity stays almost constant The maximum adsorption capacity of Pb +2 and Cd+2 are found to be 98.67 96.43mg/g, at pH= 6 and 98.71, 96.57 mg/g at pH=7 respectively with adsorbents PO/Fe3O4. The pH of the solution will influence both the aqueous chemistry and binding sites of PO/Fe3O4. Also, a change in pH causes a change in the charge profile of the Pb(II) and Cd (II) species interactions.

At lower pH values, the concentration of H+ ions far exceeds that of the metal ions from reaching the binding sites of the adsorbent caused by repulsive forces However, the metal ion removal is minimal, presumably due to enhanced competition of H+ with metal ions for the binding sites and complex formation. With the increase pH, the competing effect of H+ ions decreased and enhance the Pb (II) and Cd (II) ions could easily bind to the adsorption sites more effectively. From Fig. 11 an optimum pH value of 6 was fixed for further adsorption experiment.

Annals of R.S.C.B., ISSN:1583-6258, Vol. 25, Issue 3, 2021, Pages. 8420 - 8434
Received 16 February 2021; Accepted 08 March 2021.

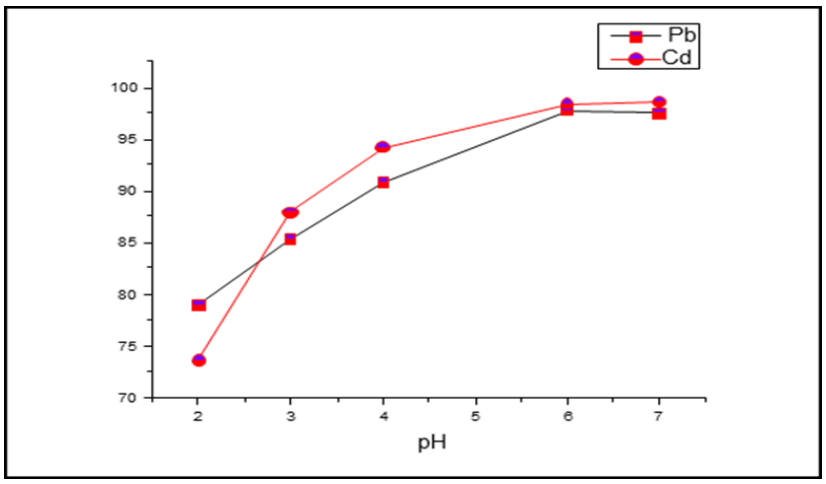

Fig. 11. Effect of pH onto sorption of Pd (II) and Cd(II) (Initial metal ion concentration = 100 mg=L, dose = 10 mg, and contact time = 30 minutes)

Influence of Contact Time on the Sorption of Pb (II) and Cd(II)

For efficient use of the adsorbents contact time is one of the significant parameters. The time dependent behaviors of the removal of Pb (II) and Cd(II) from aqueous solution by PO/Fe3O4 resin is shown in Fig. 12. The adsorption capacity increases rapidly during initial periods and further increase beyond the contact time of the initial adsorption rate was very quick which is due to5 minutes had negligible impact on the removal amount the presence of greater number of resin sites available for metal ion adsorption. More than 70 mg/g of the Pb+2 and Cd+2 were adsorbed during the first 5 minutes. As the contact time increases Pb(II) and Cd(II) elimination also increases initially but eventually reaches a more or less constant value, denoting the attainment of equilibrium. The PO/Fe3O4 Cd(II)/Pb(II) ions interactions reached equilibrium with in the first 15 minutes. Hence an optimal contact time of 15minutes was chosen for further experiments.

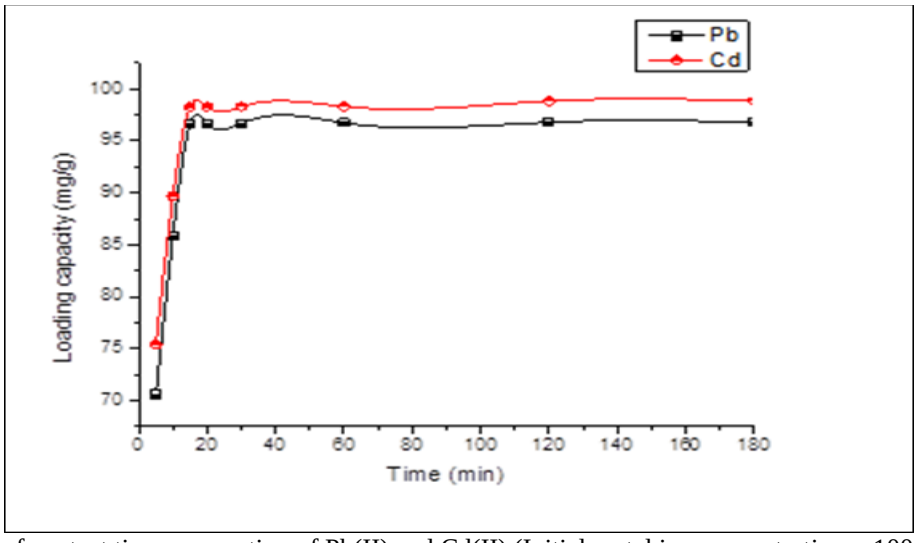

Fig. 12. Effect of contact time on sorption of Pb(II) and Cd(II) (Initial metal ion concentration = 100 mg/L, solution pH = 6.0, and adsorbent dose = 10 mg)

Influence of Adsorbent Dosage on the Sorption of Pb(II)and Cd(II)

In batch adsorption studies, the dose of PO/Fe3O4 is an important parameter as it defines the adsorption potential of PO/Fe3O4 which may be due to the availability of more binding sites and increased surface area. With an improvement in the PO dose fig (13) shown initially, the percentage removal of Cd2+ and Pb+2ions increases and then it remains constant. Since the active sites were filled at an

Annals of R.S.C.B., ISSN:1583-6258, Vol. 25, Issue 3, 2021, Pages. 8420 - 8434
Received 16 February 2021; Accepted 08 March 2021.

adsorbent dose of 10 mg; further addition of the adsorbent would not result in any significant change in the loading capacity. The optimal adsorbent dose of 10 mg was therefore fixed for other adsorption studies.

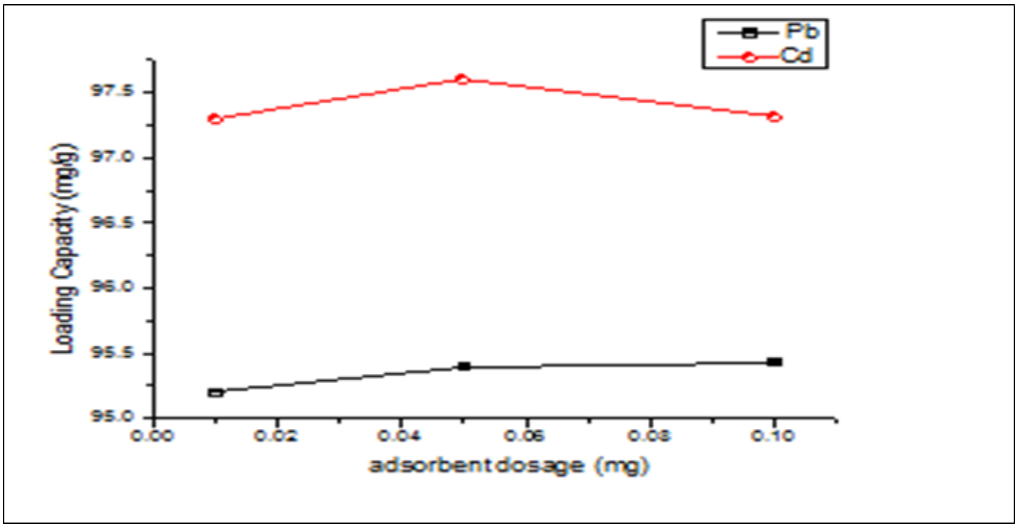

Fig. 13. Effect of adsorbent dosage onto sorption of Pb(II) and Cd(II Initial metal ion concentration = 100 mg/L, solution pH =6.0)

Desorption and Reusability

From the functional point of view, reusability is a key aspect of an adsorbent. In this job, the regeneration was performed by immersion the PO /Fe3O4 in solution. After achieving the optimum ion absorption, the polymer were then subjected to desorption by 1N HCl solution. The adsorption-desorption cycles were replicated using the same beads and the results are shown in Fig. 14. After five cycles of regeneration, the re-adsorption volume of ions remained almost constant indicating that the chelating sites on the beads were reversible. The could be repeatedly used without significantly loss in the binding affinity. The excellent reusability made it economically possible for the application of heavy metal removal from wastewater. (Lin, Tai-Lin; Lien, Hsing-Lung (2013).)

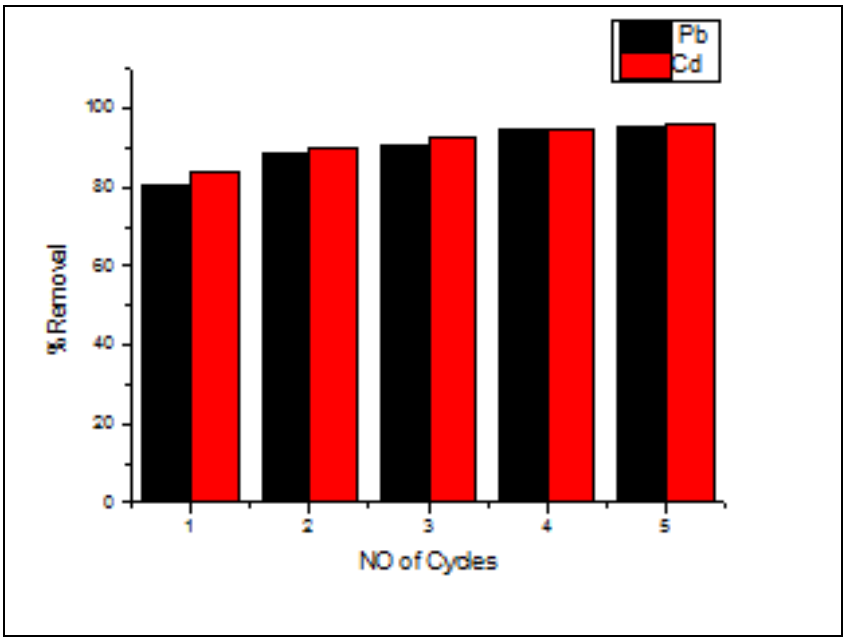

Fig. 14. Recyclability of PO/Fe3O4

Annals of R.S.C.B., ISSN:1583-6258, Vol. 25, Issue 3, 2021, Pages. 8420 - 8434
Received 16 February 2021; Accepted 08 March 2021.

DPPH Scavenging Activity

The α, α-diphenyl-β-picrylhydrazyl (DPPH) radical is a stable N-centered radical at room temperature that is commonly employed to evaluate the radical-scavenging properties of antioxidants (Xie, 2019). A lower absorbance of the reaction mixture suggests a higher DPPH radical-scavenging operation. In Figure 15, the poly amid (PO) exhibited a steady increase in scavenging DPPH free radical with the concentration increase. The scavenging efficiency of poly amid-thiourea (PO) was comparable to that of ascorbic acid, superior to butylated hydroxytoluene (BHT) at less than 1000 µg/mL. Therefore, the poly thiourea- amid (PO) have substantial DPPH radical scavenging activity

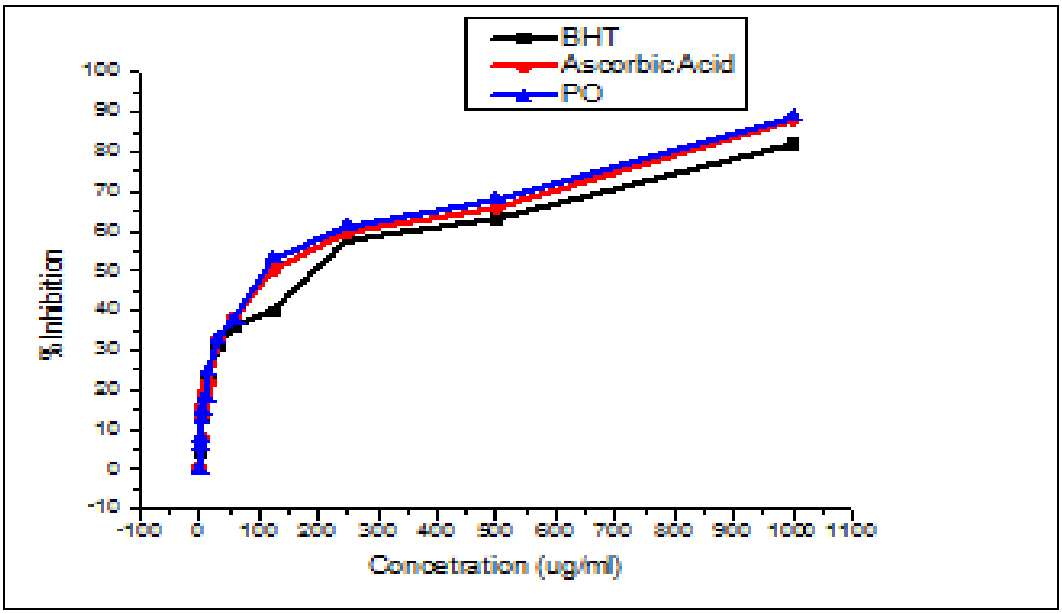

Fig. 15. DPPH radical scavenging activities of sample and control standards. Each value is expressed as a mean ± S.D (n = 3).

Conclusions

The synthesis and characterization of aromatic poly(amide -thiourea) containing thiourea and amide functions in the polymer backbone has been described. the heavy metal chelating polymer and magnetic separation are promising approaches for metal pollutant removal. In this study, both techniques were combined and a magnetic poly amid-thiourea chelating resin was produced. The resin is a type of composite polymer material a good magnetic response. The produced resin had a high Cd and Pb removal rate and also showed the resin could be regenerated using hydrochloric acid solution and was reused five times with a decent adsorption rate. The sulfur atoms of the resin had a coordinated adsorption with forming a stable coordination compound dependence. The magnetization at 300 K were consistent with the microscopic observation. The nanoparticles exhibited the superparamagnetic behavior above the blocking temperature, thus following the characteristics behavior of single domain nanoparticles. The X-ray diffraction results indicated that the Fe3O4 is in the spinel phase before and after coating. Further investigation on the nature and mechanism of the linkage between the polymer and Fe3O4 particles is ongoing and to be reported in the following articles.

References

[1] Abd Halim, A.N., & Ngaini, Z. (2016). Synthesis and bacteriostatic activities of bis (thiourea) derivatives with variable chain length. *Journal of Chemistry*, *2016*. https://doi.org/10.1155/2016/2739832

[2] Androvič, L., Drabina, P., Svobodová, M., & Sedlák, M. (2016). Polystyrene supported benzoylthiourea—pyrrolidine organocatalyst for the enantioselective Michael addition. *Tetrahedron: Asymmetry, 27*(16), 782–787. https://doi.org/10.1016/j.tetasy.2016.06.015

Annals of R.S.C.B., ISSN:1583-6258, Vol. 25, Issue 3, 2021, Pages. 8420 - 8434
Received 16 February 2021; Accepted 08 March 2021.

[3] Bharagava, R.N., Saxena, G., Mulla, S.I., & Patel, D.K. (2018). Characterization and identification of recalcitrant organic pollutants (ROPs) in tannery wastewater and its phytotoxicity evaluation for environmental safety. *Archives of environmental contamination and toxicology*, *75*(2), 259-272.

[4] Bandar, S., Anbia, M., & Salehi, S. (2021). Comparison of MnO_2 modified and unmodified magnetic Fe_3O_4 nanoparticle adsorbents and their potential to remove iron and manganese from aqueous media. *Journal of Alloys and Compounds*, *851*, 156822. https://doi.org/10.1016/j.jallcom.2020.156822

[5] Cai, W., Zhu, F., Liang, H., Jiang, Y., Tu, W., Cai, Z., & Zhou, J. (2019). Preparation of thiourea-modified magnetic chitosan composite with efficient removal efficiency for Cr (VI). *Chemical Engineering Research and Design*, *144*, 150-158. https://doi.org/10.1016/j.cherd.2019.01.031

[6] Chen, D., Liu, C., Tang, J., Luo, L., & Yu, G. (2019). *Organic polymers.* Polymer Chemistry, 1–12.

[7] Dlamini, C.L., De Kock, L.A., Kefeni, K.K., Mamba, B.B., & Msagati, T.A.M. (2020). Novel hybrid metal loaded chelating resins for removal of toxic metals from acid mine drainage. *Water Science and Technology*, *81*(12), 2568-2584. https://doi.org/10.2166/wst.2020.285

[8] Goutam, S.P., Saxena, G., Singh, V., Yadav, A.K., Bharagava, R.N., & Thapa, K.B. (2018). Green synthesis of TiO2 nanoparticles using leaf extract of Jatropha curcas L. for photocatalytic degradation of tannery wastewater. *Chemical Engineering Journal*, *336*, 386-396.

[9] Fu, Y., Yu, W., Zhang, W., Huang, Q., Yan, J., Pan, C., & Yu, G. (2018). Sulfur-rich covalent triazine polymer nanospheres for environmental mercury removal and detection. *Polymer Chemistry*, *9*(30), 4125-4131.

[10] Hajibeygi, M., Shafiei-Navid, S., Shabanian, M., & Vahabi, H. (2018). Novel poly (amide-azomethine) nanocomposites reinforced with polyacrylic acid-co-2-acrylamido-2-methylpropanesulfonic acid modified LDH: Synthesis and properties. *Applied Clay Science*, *157*, 165-176. https://doi.org/10.1016/j.clay.2018.03.004

[11] Huang, X., Cao, X., Wang, W., Zhong, H., & Cao, Z. (2017). Preparation of a novel resin with acyl and thiourea groups and its properties for Cu (II) removal from aqueous solution. *Journal of environmental management*, *204*, 264-271. https://doi.org/10.1016/j.jenvman.2017.09.007

[12] Lin, T.L., & Lien, H.L. (2013). Effective and selective recovery of precious metals by thiourea modified magnetic nanoparticles. *International journal of molecular sciences*, *14*(5), 9834-9847. https://doi.org/10.3390/ijms14059834

[13] Li, X., Liu, G., Yan, W., Chu, P.K., Yeung, K.W.K., Wu, S., & Xu, Z. (2012). Preparation of Fe3O4/poly (styrene-butyl acrylate-[2-(methacryloxy)ethyl] trimethylammonium chloride) by emulsifier-free emulsion polymerization and its interaction with DNA. *Journal of Magnetism and Magnetic Materials*, *324*(7), 1410–1418. https://doi.org/10.1016/j.jmmm.2011.11.056

[14] Kirupha, S.D., Murugesan, A., Vidhyadevi, T., Baskaralingam, P., Sivanesan, S., & Ravikumar, L. (2012). Novel polymeric adsorbents bearing amide, pyridyl, azomethine and thiourea binding sites for the removal of Cu (II) and Pb (II) ions from aqueous solution. *Separation Science and Technology*, *48*(2), 254-262. https://doi.org/10.1080/01496395.2012.681745

[15] Murugesan, A., Vidhyadevi, T., Kalaivani, S.S., Thiruvengadaravi, K.V., Ravikumar, L., Anuradha, C.D., & Sivanesan, S. (2014). Modelling of lead (II) ion adsorption onto poly (thiourea imine) functionalized chelating resin using response surface methodology (RSM). *Journal of Water Process Engineering*, *3*, 132-143. https://doi.org/10.1016/j.jwpe.2014.06.004

[16] Mahdavi, M., Ahmad, M.B., Haron, M.J., Namvar, F., Nadi, B., Rahman, M.Z.A., & Amin, J. (2013). Synthesis, surface modification and characterisation of biocompatible magnetic iron oxide nanoparticles for biomedical applications. *Molecules*, *18*(7), 7533-7548.

[17] Magdalena, A.G., Silva, I.M.B., Marques, R.F.C., Pipi, A.R.F., Lisboa-Filho, P.N., & Jafelicci Jr, M. (2018). EDTA-functionalized Fe_3O_4 nanoparticles. *Journal of Physics and Chemistry of Solids*, *113*, 5-10. https://doi.org/10.1016/j.jpcs.2017.10.002

[18] Okuniewski, A., Rosiak, D., Chojnacki, J., & Becker, B. (2015). Coordination polymers and molecular

Annals of R.S.C.B., ISSN:1583-6258, Vol. 25, Issue 3, 2021, Pages. 8420 - 8434
Received 16 February 2021; Accepted 08 March 2021.

structures among complexes of mercury (II) halides with selected 1-benzoylthioureas. *Polyhedron*, *90*, 47-57. https://doi.org/10.1016/j.poly.2015.01.035

[19] Pearson, R.G. (1968). Hard and soft acids and bases, HSAB, part 1: Fundamental principles. *Journal of Chemical Education*, *45*(9), 581. https://doi.org/10.1021/ed045p581

[20] Şenol, D., & Kaya, İ. (2017). Synthesis and characterization of azomethine polymers containing ether and ester groups. *Journal of Saudi Chemical Society*, *21*(5), 505–516. https://doi.org/10.1016/j.jscs.2015.05.006

[21] Saxena, G., & Bharagava, R.N. (2017). *Organic and inorganic pollutants in industrial wastes, their ecotoxicological effects, health hazards and bioremediation approaches.* Environmental pollutants and their bioremediation approaches, 1st edn. CRC Press, Taylor & Francis Group, Boca Raton, 23-56.

[22] Liang, W., Li, M., Jiang, S., Ali, A., Zhang, Z., & Li, R. (2019). Polyamine-co-2, 6-diaminopyridine covalently bonded on chitosan for the adsorptive removal of Hg (II) ions from aqueous solution. *International journal of biological macromolecules*, *130*, 853-862.

[23] Wei, S., Zhu, Y., Zhang, Y., & Xu, J. (2006). Preparation and characterization of hyperbranched aromatic polyamides/Fe3O4 magnetic nanocomposite. *Reactive and Functional Polymers*, *66*(11), 1272-1277. https://doi.org/10.1016/j.reactfunctpolym.2006.03.008

[24] Xie, K., He, X., Chen, K., Chen, J., Sakao, K., & Hou, D. X. (2019). Antioxidant properties of a traditional vine tea, Ampelopsis grossedentata. *Antioxidants*, *8*(8), 295. https://doi.org/10.3390/antiox8080295

[25] Zhou, S., Zhang, M., Wang, R., Ping, J., Zhang, X., Zhao, N., & Fan, X. (2017). Synthesis and characterization of new aramids based on o -(m -triphenyl)-terephthaloyl chloride and m -(m -triphenyl)-isophthaloyl chloride. *Polymer*, *109*, 49–57.

[26] Sykes, P. (2000). *A guidebook to mechanism in organic chemistry, 6th.* Ed., Longman, U.K.

[27] RE-Lin, Tai-Lin; Lien, Hsing-Lung (2013). Effective and Selective Recovery of Precious Metals by Thiourea Modified Magnetic Nanoparticles. *International Journal of Molecular Sciences*, *14*(5), 9834–9847. https://doi.org/10.3390/ijms14059834